IEEE Access
Multidisciplinary | Rapid Review | Open Access Journal

Received September 26, 2019, accepted October 6, 2019, date of publication October 15, 2019, date of current version October 28, 2019.

Digital Object Identifier 10.1109/ACCESS.2019.2947537

Saliency-Guided Repetition Detection From Facade Point Clouds

WEN HAO, WEI LIANG, YINGHUI WANG, MINGHUA ZHAO, AND YE LI
Institute of Computer Science and Engineering, Xi'an University of Technology, Xi'an 710048, China

Corresponding author: Wen Hao (haowensxsf@163.com)

This work was supported in part by the National Natural Science Foundation of China under Grant 61602373, in part by the Shaanxi Science Research Plan under Grant 2018JQ6049, Grant 2018JQ6055, and Grant 2019JQ-740, and in part by the Key Laboratory Research Project of Shaanxi Provincial Education Department under Grant 18JS078.

ABSTRACT We present a saliency-guided algorithm for detecting the locations of repetitive structures on building facades. First, the global and local saliencies of each point are determined by measuring the global rarity and the local distinctness. The saliency map is utilized to adaptively extract the salient points. Second, the salient points are vertically sliced. A curve can be derived by counting the total number of points in each slice. Then, the curve is converted into a square wave to locate the vertical splitting position. Next, each segment is horizontally sliced, similar to the vertical splitting. The salient points are partitioned into repetitive candidates after the vertical and horizontal splitting. Finally, the repetitive candidates are refined according to the similarity of the neighborhood and the regularity of the arrangement. The experimental results demonstrate that our method can quickly and effectively extract repetitions from facade point clouds.

INDEX TERMS Saliency detection, facade point clouds, repetitive structure detection, vertical/horizontal splitting, refinement.

I. INTRODUCTION

Windows are important elements of a building facade. Accurate detection of 3D facade elements has become highly important for urban building modeling because the reconstructed models have been widely used for many important applications, such as virtual tourism, urban planning, and entertainment. There is an extensive literature on repetitive structure detection methods, which range from image-based methods [1]–[3] to 3D point-based methods [4]–[6]. Due to the loss of three-dimensional information in two-dimensional imaging and the inevitable influences of illumination, reflections and occlusions, detecting repetitive structures from images remains difficult. Recent advances in terrestrial laser scanning (TLS) provide a convenient approach for quickly collecting 3D point clouds of a building facade. Three-dimensional point clouds with high density and high accuracy can express the geometric details of objects. Several point cloud-based methods, such as slice-based methods [5], [6] and boundary-based methods [7], [8], were proposed for extracting the repetitions from facade point clouds. A data gap appears where the laser beam does not return a signal due to window glass or other openings. In order to detect the opening areas across the facade, slice-based methods must segment the point cloud of each planar facade using Random sample consensus (RANSAC) or a region growing method in advance. For the boundary-based methods, incorrect boundary points are always detected due to occlusion and poor scan quality, which greatly increase the difficulty of window detection.

To address the difficulty of window detection from facade point clouds, we propose a novel approach to detect windows based on saliency maps. Saliency is closely related to selective processing in the human visual system, which is used a measure of regional importance for 3D models. Saliency has been extensively studied in recent years. Due to the disorderliness and the absence of topological information regarding the point connectivity, the existing mesh saliency methods [9]–[11] cannot be directly applied to unorganized point sets. Shtrom *et al.* [12] proposed a saliency detection method for 3D point sets that is based on identifying the distinct points using a multi-level approach. The distinctiveness of each point is computed by comparing the point's local descriptor to all other descriptors that are sufficiently close in the descriptor space. Ponjou *et al.* [13] proposed a cluster-based approach for computing the saliency of the point set. Both used Fast Point Feature Histogram (FPFH) as the local shape descriptor. Guo *et al.* [14] presented a point cloud

The associate editor coordinating the review of this manuscript and approving it for publication was Songwen Pei.

saliency detection method that employs principal component analysis (PCA) in a sigma-set feature space. Saliency detection in point clouds has been used in viewpoint selection, producing the most informative tour, 3D model simplification and key point detection. Although saliency maps have been used in many applications in recent years, very little work has utilized saliency maps to detect repetitions on building facades.

In this paper, we concentrate on extracting repetitive structures from facade point clouds based on point saliency. We propose a robust method for the selection of a very small fraction of the facade point clouds, namely, for extracting the point clouds that represent the window frames on the facade. Toward this objective, a 3D saliency measure is defined for extracting the salient points from facade point clouds. The main contributions of the paper are summarized as follows:

1) Instead of detecting inner boundaries or the openings to locate the repetitions, a saliency-guided method is proposed to detect the locations of repetitions. The salient points that correspond to the repetitive structures are extracted based on the saliency maps. Regardless of the diversity of window type and quality of scanned data, the extracted salient points have strong uniqueness and invariance that capture the regions of repetitive structures effectively.

2) Windows and doors are important elements that often correspond to repeatable structures on building facades. A novel slicing-based method is proposed for segmenting the salient points into repetitive candidates effectively. Unlike finding the local minima as the splitting locations, a curve, which is derived from the number of points of each slice, is converted into a binary form for splitting repetitions accurately. The slices with point number less than a certain threshold are removed that reduces the influence of noise effectively. In addition, a refinement that is based on the similarity of structure and neighborhood is proposed for guaranteeing the detection accuracy.

The remainder of the paper is organized as follows. Section II presents a brief review of repetition detection. Section III presents the process of extracting repetitions from building point clouds based on point saliency. The detailed steps of repetition extraction are proposed in Section IV. Experimental results are presented in Section V. The limitations of our method and proposals for future research are discussed in the last section.

II. RELATED WORKS

The extraction of repetitions from facades has been studied in recent years. Many methods for repetitive structure detection have been introduced recently, which fall into two main categories: image-based methods and point cloud-based methods.

A. IMAGE-BASED METHODS

Due to the convenience of acquisition and the rich information, image-based methods play an important role in repetition detection. Müller *et al.* [15] segmented a facade into tiles and recursively split each tile based on an edge map to extract windows. Shape grammar rules are used to identify repetitive windows from a single, high-quality photograph of a facade. Wu *et al.* [16] exploited boundary selection for dense repetition detection. They maximized local symmetries and separated repetition groups via the evaluation of the local repetition quality conditionally for repetition intervals. Mathias *et al.* [17] proposed a three-layered system for semantic segmentation of building facades, in which three levels of abstraction are represented in facade images: segments, objects and architectural elements. Lian *et al.* [18] employed the color clustering method to automatically derive candidate templates. Then, an adaptive region descriptor and a Bayesian network were used for repetition detection and occlusion inference. Xiao *et al.* [19] extracted horizontal and vertical fiducial lines to detect repetitions in rectified facade images based on the observation that repetitions of a building facade are typically horizontally and vertically aligned. Cohen *et al.* [20] presented a greedy dynamic programming-based algorithm that imposes very few but common constraints on the parsing, while also respecting detected symmetries and repetitions, along with image edges. Symmetry information is used to efficiently address large occluded areas and to recover plausible facade images with minimal occlusions. In these methods, facade images should be rectified in advance. With the development of airborne oblique photogrammetry, many methods were proposed for detecting windows from aerial images. Yang *et al.* [21] extracted facade regions using straight line segments based on a multi-level feature extraction procedure. The method is severely affected by the detection accuracy of the line segments.

The acquisition of facade images always suffers from occlusions, reflections and illumination changes. In addition, the image to be detected should be in a fronto-parallel view. Due to these variances and corruption, detecting windows from a facade image remains challenging.

B. POINT CLOUD-BASED METHODS

Since windows have a low laser reflection rate, there are typically no or few laser points that represent windows in 3D point clouds. Based on this observation, Zolanvari and Laefer [5] and Zolanvari *et al.* [6] introduced a slicing method to detect windows from building facades. After extracting the building facades using the RANSAC algorithm, each facade is horizontally and vertically sliced. Gaps are detected by identifying the points that have distances that exceed twice the median distance of points along that line. The number of slices influences the detection accuracy.

Pu and Vosselman [7] classified the boundary points of a building facade into outer boundaries and inner boundaries. The inner boundaries were used to extract the windows. Similar to Pu and Vosselman [7], Peethambaran and Wang [8] split the building facade into horizontal and vertical tiles using a weighted point count function that is defined over the window or door boundaries. Incorrect boundary points are always detected due to occlusions and poor scan quality,

which substantially increases the difficulty of window extraction. Friedman and Stamos [22] extracted the repeated architectural features through Fourier analysis after identifying the major plane of building. They assumed that the distances between the repetitions are consistent. After segmenting the urban point clouds using a region growing method, Mesolongitis and Stamos [23] adapted a local lattice fitting and lattice voting scheme for lattice detection. The method assumes regular window patterns on the facade and projects the 3D points onto a 2D binary orthographic point occupancy map. Aijazi *et al.* [24] also projected the point clouds of a facade onto a 2D plane that was parallel to the building facade. After point inversion within a watertight boundary, windows were segmented out based on the geometrical information. The 2D projection prior to the window extraction will inevitably lead to a loss of precision. Li *et al.* [25] introduced a hierarchical approach that uses the semantic and underlying structures of urban facades for modeling 3D building facades from TLS point cloud data. The facade points are segmented into multiple 2.5D depth planes, among which the facade elements are accurately detected by collectively using semantic segmentation, arrangement priors of facade elements, and machine learning recognition. Hao *et al.* [26] extracted the window frames and selected the incomplete windows first. Then, a template-matching method that relies on the similarity and repetitiveness of the windows is proposed to recover the details on building facades.

Most point cloud-based methods must segment the buildings in advance or based on the extraction of interior boundaries. However, this process is sensitive to the quality of the raw point cloud data. Saliency detection for 3D point clouds can be regarded as the identification of perceptually important regions that are unique with respect to their surrounding regions. Regardless of the density distribution of the scanned data, a salient area has strong uniqueness and invariance. Due to the advantages of saliency, we present a saliency-guided method to detect repetitive structures from facade point clouds. The frames of repetitive structures that consist of salient points are extracted based on the saliency maps. A novel slicing method is designed to partition the salient points into repetitive candidates. A refinement that is based on the neighborhood similarity and the arrangement regularity is also proposed to guarantee the correctness of detection. The proposed saliency-guided algorithm can generate satisfactory results for imperfect point clouds by avoiding facade segmentation and boundary extraction.

III. ALGORITHM OVERVIEW

The process of the repetitive structure detection approach is described using a flowchart in Fig. 1.

1) Saliency map construction. We define a 3D saliency measure for extracting salient points from facade point clouds. Considering the human visual perception mechanism, the global-distinct feature is defined as the dissimilarity of the normals between each point and the building facade. The local-distinct feature is defined as the local dissimilarity of

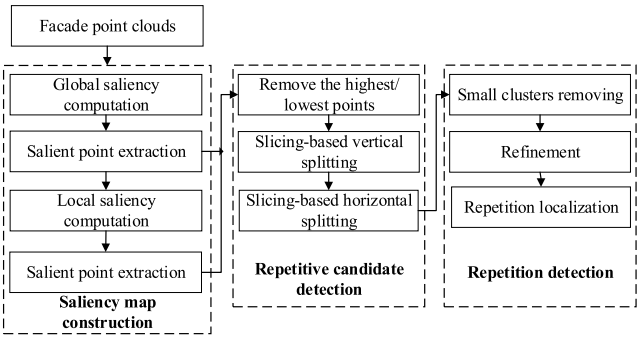

FIGURE 1. Overview of the proposed method.

geometric information by using the point descriptor FPFH. After constructing the global/local saliency map of the facade point clouds, the salient points that belong to the frames of the repetitions are extracted.

2) Repetitive candidate detection. The high saliency points represent the frames of the repetitive structures on the facade. The salient points are vertically sliced. The number of points in each slice is recorded and a curve is derived from the number of points of each slice. To detect the splitting position accurately, the curve that is derived from the number of points is converted into binary form. The '1-0' transactions are employed as the splitting locations. A similar operation is performed along the horizontal direction. After the vertical and horizontal splitting, the salient points are segmented into repetitive candidates.

3) Repetition detection. Due to the occlusion and noise, the repetitive elements may be over segmented into several parts. An optimization process that is based on the similarity and regularity is conducted to improve the accuracy of repetition detection. Each repetition is localized after the refinement.

IV. SALIENCY GUIDED WINDOW REPETITION DETECTION

A. SALIENCY MAP CONSTRUCTION AND SALIENT POINT EXTRACTION

According to the attention mechanism of human beings, the salient regions are often the regions in which drastic changes in local features occur and that have a relative scarcity of point cloud data.

Wang *et al.* [27] constructed a saliency map on 3D point clouds by computing the dominant normal vector of the point cloud via K-means clustering, and projecting the distance between each normal vector and the dominant normal vector into a hyperbolic tangent function space. In this paper, we extend Wang's method to construct a saliency map on 3D point clouds directly. Compared with Wang's saliency map construction method, our method not only considers the global rarity (the relative scarcity of normals), but also the local distinctness (the variation of local geometric features).

1) GLOBAL SALIENCY

The global saliency measures the global rarity of a point. The global rarity is used to detect entire unique regions.

For a vertex in a facade point cloud, the less similar the other vertices are, the stronger its global saliency. In this paper, the global saliency is used to highlight the dissimilarity of normals between each point and the building facade. The point normal and the dominant normal of a building facade can be computed via PCA. The dominant normal of each building facade is determined by using the matrix of the points in the facade. The matrix for a facade point cloud is constructed as follows:

$$M = \frac{1}{N}\sum_{i=1}^{N}(p_i - \bar{p})(p_i - \bar{p})^T \tag{1}$$

where $\bar{p}$ denotes the center of the facade point cloud and N denotes the total number of points in the facade point cloud. Through eigenvalue decomposition of M, three eigenvalues $\lambda_0, \lambda_1, \lambda_2(\lambda_0 \geq \lambda_1 \geq \lambda_2)$ and the associated eigenvectors e_0, e_1, e_2 are obtained.

The dominant normal vector of the facade point cloud is e_2, which is the eigenvector associated with the smallest eigenvalue of M.

Similar to Wang's method, the global saliency $S_{global}(p_i)$ of point p_i is measured by projecting the distance of each point's normal vector into a hyperbolic tangent function space. The salient points are extracted by using:

$$P_i = \begin{cases} 1, & S_{global}(p_i) > \alpha \\ 0, & S_{global}(p_i) < \alpha \end{cases} \tag{2}$$

If the global saliency $S_{global}(p_i)$ of point p_i is larger than the threshold α, point p_i is a salient point; otherwise, p_i is a non-salient point.

Fig. 2(a) shows facade point cloud 1 and Fig. 2(b) shows the saliency map of facade point cloud 1. The salient points, which belong to the frames of repetitive structures, are colored in red. As shown in Fig. 2(c), the salient points are extracted based on the global saliency.

2) LOCAL SALIENCY

A point is distinct if it differs from its local surroundings. To calculate the local distinctness of each point, a descriptor is needed to characterize the local geometric features. FPFH [28] has satisfactory expressive power of the local shape geometry, which is robust to noise and to sampling density. FPFH captures the relative angular directions of the normals with respect to one another. FPFH can be used to compute the similarity between a point and its neighborhoods. FPFH is used to compute the local saliency of facade point clouds.

Given two points p_i and p_j, the χ^2 dissimilarity measure between them is defined as:

$$D_{\chi^2}(p_i, p_j) = \sum_{n=0}^{N}\frac{(FPFH_n(p_i) - FPFH_n(p_j))^2}{FPFH_n(p_i) + FPFH_n(p_j)} \tag{3}$$

where N is the number of bins in the FPFH and $FPFH_n(p_i)$ denotes the *n-th* bin of the histogram of p_i. The local

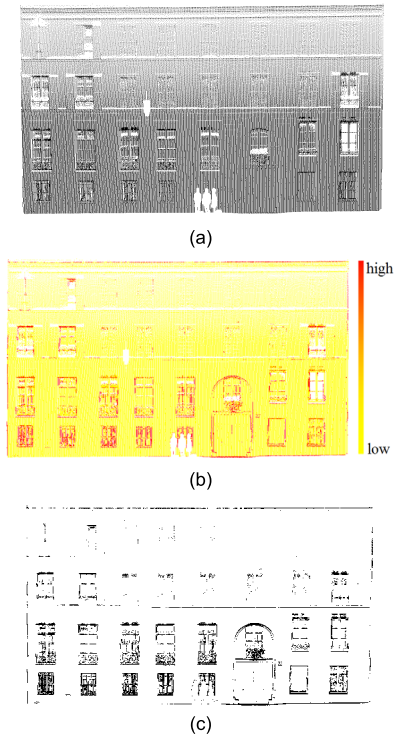

FIGURE 2. Illustration of global salient map construction and salient point extraction. (a) Facade point cloud 1. (b) The constructed global saliency map. (c) The salient points that were extracted based on the global saliency.

dissimilarity measure between p_i and p_j is defined as:

$$d_H(p_i, p_j) = D_{\chi^2}(p_i, p_j) \cdot \|p_i - p_j\| \tag{4}$$

where $\|p_i - p_j\|$ denotes the distance between point p_i and p_j. The local saliency is computed on a small neighborhood. Suppose p_i is a point in the facade point cloud and $\{p_1, p_2, \cdots p_k\}$ are the k-nearest neighboring points of p_i. The local distinctness of point p_i is defined as the weighted sum of the dissimilarities with its surrounding points:

$$S_{local}(p_i) = 1 - \exp\left(-\frac{1}{k}\sum_{j=0}^{k} d_H(p_i, p_j)\right) \tag{5}$$

where k is set to 30 in our experiments.

The salient points are extracted by using:

$$P_i = \begin{cases} 1, & S_{local}(p_i) > \beta \\ 0, & S_{local}(p_i) < \beta \end{cases} \tag{6}$$

If the local saliency $S_{local}(p_i)$ of point p_i is larger than the threshold β, point p_i is a salient point; otherwise, p_i is a non-salient point.

Fig. 3(a) shows the local saliency map of facade point cloud 1 and Fig. 3(b) shows the salient points that are extracted according to the local saliency. Fig. 3(c) shows the salient points that are merged based on the global and local saliency.

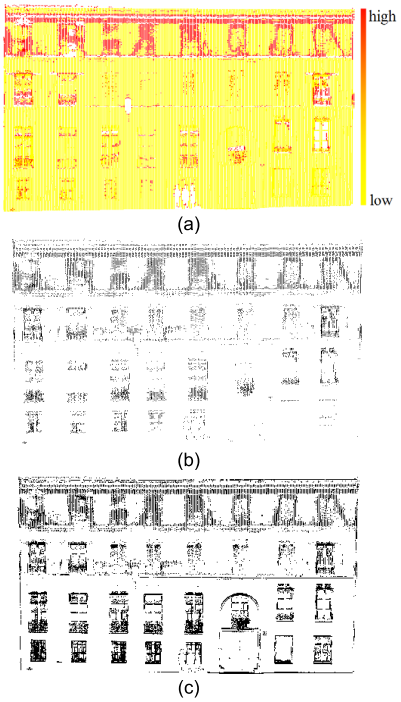

FIGURE 3. Illustration of local saliency map construction and salient point extraction. (a) The constructed local saliency map. (b) The salient points that are extracted based on the local saliency. (c) The merged salient points.

B. INITIAL SPLITTING OF REPETITIVE STRUCTURES

The salient points that were extracted in the previous step represent the frames of the repetitive structures. The highest and lowest salient points are removed because these points typically correspond to wall eaves or the points where the wall connects to the ground.

Observing that repetitions are typically horizontally and vertically aligned and thus can be localized by the horizontal and vertical lines along the repetition frames, we propose a slicing-based method for dividing the salient points into different parts.

The salient points are first cut into a sequence of slices $s = \{s_1, s_2, s_3 \cdots s_N\}$ vertically by dividing by the slice number N. Let $x_{\max}, y_{\max}, x_{\min}$, and $y_{\min}$ denote the maximum and minimum x and y values of the salient points that are extracted from the facade. If $(x_{\max}\text{-}\ x_{\min}) < (y_{\max}\text{-}\ y_{\min})$, the facade is sliced along the y-axis. Otherwise, the facade is sliced along the x-axis. The width of each slice is defined as $\Delta y = \frac{y_{\max}-y_{\min}}{N}$. The number of points in each slice is recorded. For a point p_j, we define:

$$f_y(p_j) = \begin{cases} 1, & y_{p_j} \in [y_{\min}+i*\Delta y, y_{\min}+(i+1)*\Delta y] \\ 0, & otherwise \end{cases} \quad (7)$$

where i is the index of slice s_i. The number of points $T(s_i)$ within a slice s_i is accumulated as:

$$T(s_i) = \sum_{j=0}^{n} f_y(p_j) \quad (8)$$

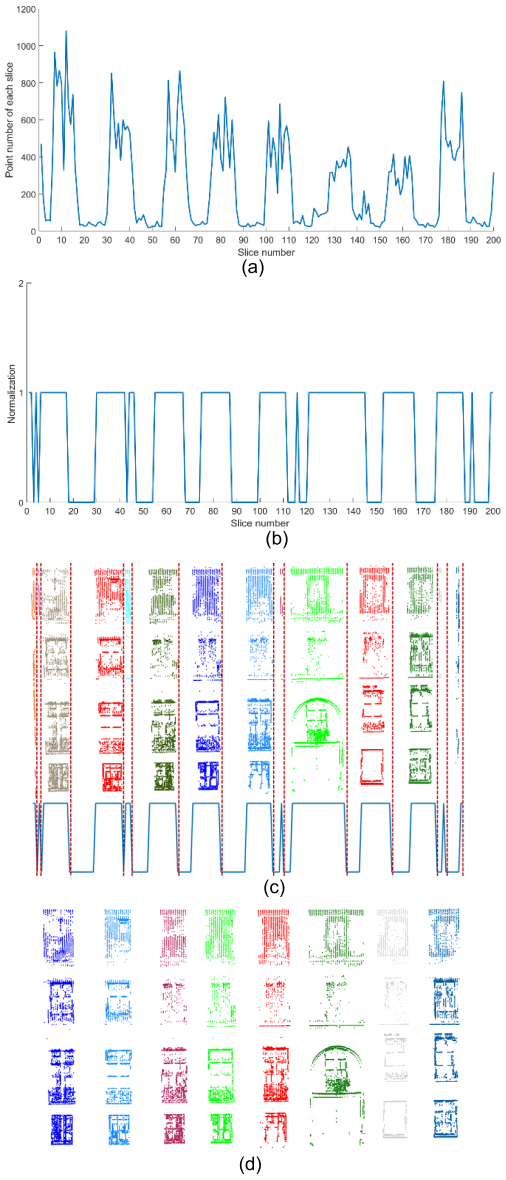

FIGURE 4. Diagram of vertical splitting. (a)The curve that was derived from the number of points of each slice. (b) The binary form. (c) The vertical splitting lines that were inserted at the '1-0' transition. (d) The vertical splitting result.

where n is the total number of salient points. A repetitive characteristic curve can be obtained by using (8). The curve of salient points in facade 1 is plotted in Fig. 4(a). The horizontal axis in Fig. 4(a) corresponds to the slice number and the vertical axis to the number of points of each slice. In frequency space, periodic functions have salient minima at the frequencies of the period of the signal. The curve is converted into a square wave to determine the splitting position. To fit a square wave, the number of points of each slice is converted into a binary function by setting all values above a threshold γ as 1 and all values below it as 0. The binary splitting function is formulated as:

$$F_i = \begin{cases} 1, & C(s_i) > \gamma \\ 0, & C(s_i) < \gamma \end{cases} \quad (9)$$

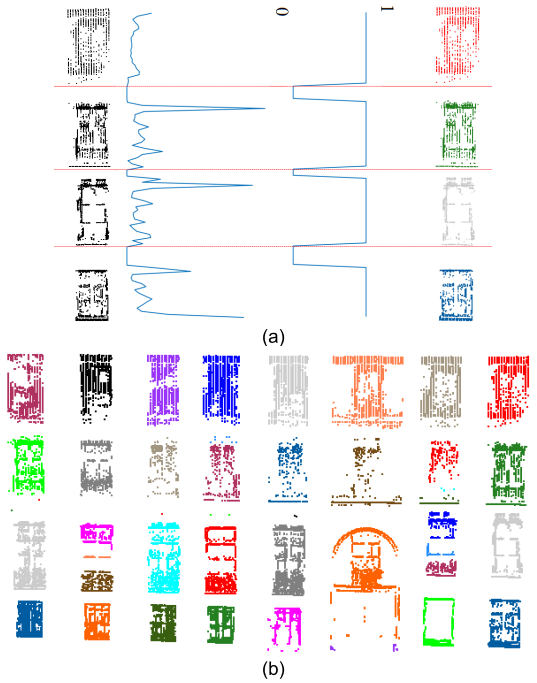

FIGURE 5. Horizontal splitting of facade point cloud 1. (a) The horizontal repetition splitting for the last column. (b) The initial splitting result.

where γ denotes the threshold of number of points, which depends on the facades to be split.

Fig. 4(b) shows the square wave fit from Fig. 4(a). In the binary form, we use '1-0' transition to determine the splitting position. The red dotted lines in Fig. 4(c) represent the initial splitting positions of vertical splitting. A slice is labelled with 0 if the number of points in the slice is smaller than γ. The slices that are labelled with 0 are removed in the process of vertical splitting. After splitting, the short and narrow slices are removed. Fig. 4(d) shows the vertical splitting results after removing the narrow slices. Different segments are marked with different colors.

The similar operation is performed along the horizontal direction. Each window column is re-sliced along the z-axis. Considering the rightmost column window of facade point cloud 1 as an example, the total number of points in each slice is recorded and a repetitive curve is derived from the numbers of points in the slices (the left curve in Fig. 5(a)). Then, the curve is converted into binary form (the right curve in Fig. 5(a)). The '1-0' transitions are regarded as the splitting locations. Fig. 5(b) shows the initial splitting result and different parts are marked with different colors. For the binary function, the threshold γ is always set as 0 in the horizontal splitting.

C. REFINEMENT

After the vertical/horizontal splitting, small clusters are removed. A window may be split into several parts due to improper splitting. According to the observation, the adjacent windows have similarities. We further refine the splitting result due to the structure matching and the proximity relationship.

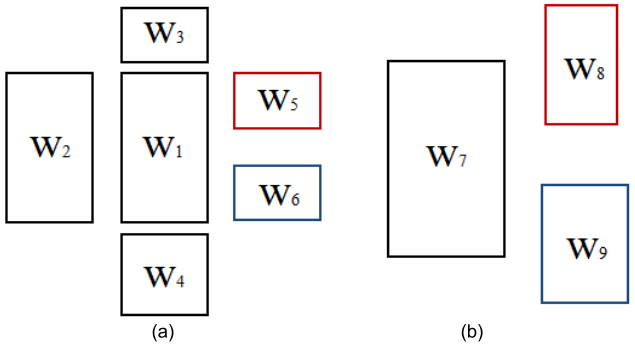

FIGURE 6. Diagram of the splitting refinement. (a) W_5 and W_6 should be merged into one part. (b) W_8 and W_9 should not be merged.

Four neighborhoods (the top, bottom, left, and right) of each candidate are recorded. If a candidate encounters two or more neighbors on one side, the structures (width or height) of the candidates should be compared. If the candidate and its neighbors are of similar width or height, we should judge whether the neighbors are contained in the vertical/horizontal range of the candidate. If so, the neighbors should be combined into a part; otherwise, the neighbors should not be combined. If the candidate and its neighbors are of dissimilar structure, the neighbors should not be combined.

As shown in Fig. 6(a), W_2, W_3, and W_4 denote the left, top, and bottom neighbors of W_1. W_5 and W_6 denote the right neighbors of W_1. As we can see, W_5 and W_6 are of similar width to W_1. In addition, W_5 and W_6 are in the vertical range of W_1. Therefore, W_5 and W_6 should be combined into a part. W_8 and W_9 in Fig. 6(b) are also the right neighbors of W_7. However, they differ substantially in terms of structure and they are not in the vertical range of W_7. Therefore, W_8 and W_9 should not be merged into a part.

As illustrated in Fig. 7(a), a window in the red dotted frame is split into two parts. Due to the similarity of the adjacent windows, they are combined into a single part (red frames in Fig. 7(b)). The incorrect detections in the red dotted frames can be eliminated in the rectification step. The detected repetitions are represented by red nodes in Fig. 7(c).

V. EXPERIMENTAL RESULTS

A. RESULTS ON DATA SETS

The proposed algorithms were programmed with PCL [29]. All the experiments in this paper were carried out on a PC with an Intel Core i7-4790, CPU 3.6 GHz, 16G memory.

Facades 1-3 are the facade point clouds that were extracted from dataset Paris-rue-Cassette [30], which was acquired using the STEREOPOLIS II MLS system. Facade point cloud 4 represents the library wall in Xi'an University of Technology, which was acquired using a Topcon GLS-1500 scanner.

In our experiments, the width of each slice is set as 0.1 for all experiments. The proposed saliency computation

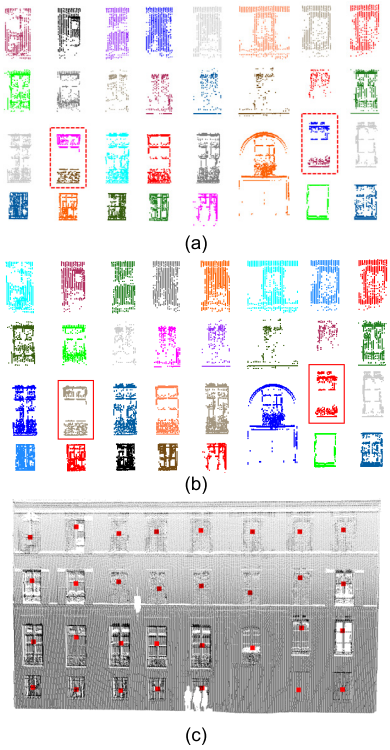

FIGURE 7. Repetition detection on facade point cloud 1 after refinement. (a)The initial splitting result. (b) The refinement result. (c) The detected windows.

TABLE 1. Parameters and thresholds.

Datasets	Global saliency α	Local saliency β
facade point cloud 1	0.6	0.9
facade point cloud 2	0.6	0.9
facade point cloud 3	0.6	0.9
facade point cloud 4	0.5	0.9

algorithm depends on two parameters: the thresholds of global saliency α and local saliency β. The parameter settings of the four datasets are listed in Table 1. The experimental results demonstrate that more extracted salient points do not yield superior results. According to the experiments, the value of the threshold α should be set according to the point density of facade point cloud. For facade point clouds 1-3, the threshold of global saliency α is set as 0.6 since the points of windows on these facades have high point density. For facade point cloud 4, the threshold of global saliency α is set as 0.5 since the facade point clouds are relatively sparse. The threshold of local saliency β is set to 0.9 for all experiments. The threshold number of points γ depends on the building facade.

According to Fig. 8, the facades that contain multiple groups of repetitive structures are successfully extracted using our method. Fig. 8(a) shows facade point cloud 3. Fig. 8(b) shows the salient points that are based on the saliency map construction. Fig. 8(c) shows the initial vertical partition result of the salient points. A similar operation is

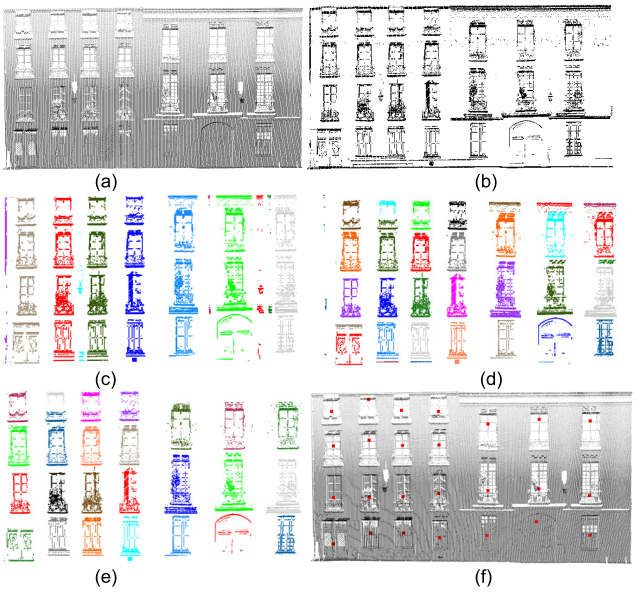

FIGURE 8. Repetition extraction from facade point cloud 2. (a) Facade point cloud 2. (b) The salient points. (c) The vertical splitting. (d) The horizontal splitting. (e) The extracted repetitive structures. (f) The detected windows.

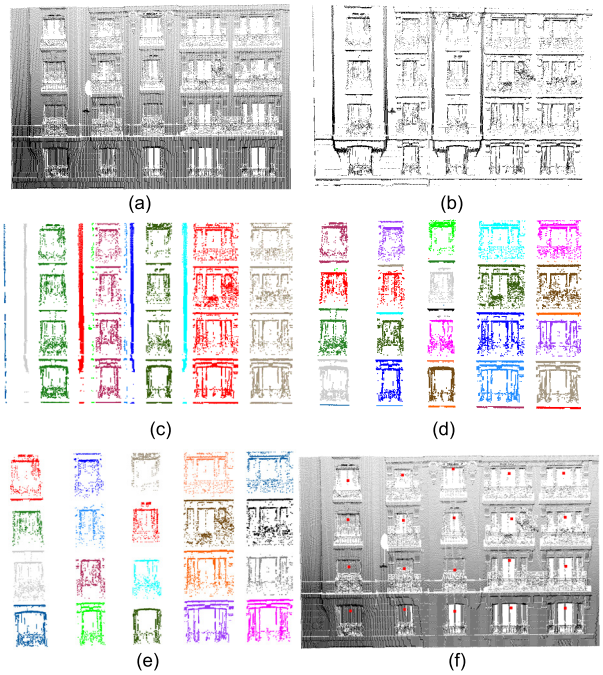

FIGURE 9. Repetition extraction from facade point cloud 3. (a) Facade point cloud 3. (b) The salient points. (c) The vertical splitting. (d) The horizontal splitting. (e) The extracted repetitive structures. (f) The detected windows.

conducted along the horizontal direction. The initial segmentation result is shown in Fig. 8(d). After removing the small clusters, the repetitive candidates are marked with different colors (Fig. 8(e)). Each detected repetition is represented by its center (red points in Fig. 8(f)).

Fig. 9(a) shows facade point cloud 3 and Fig. 9(b) shows the salient points that are based on the global and local

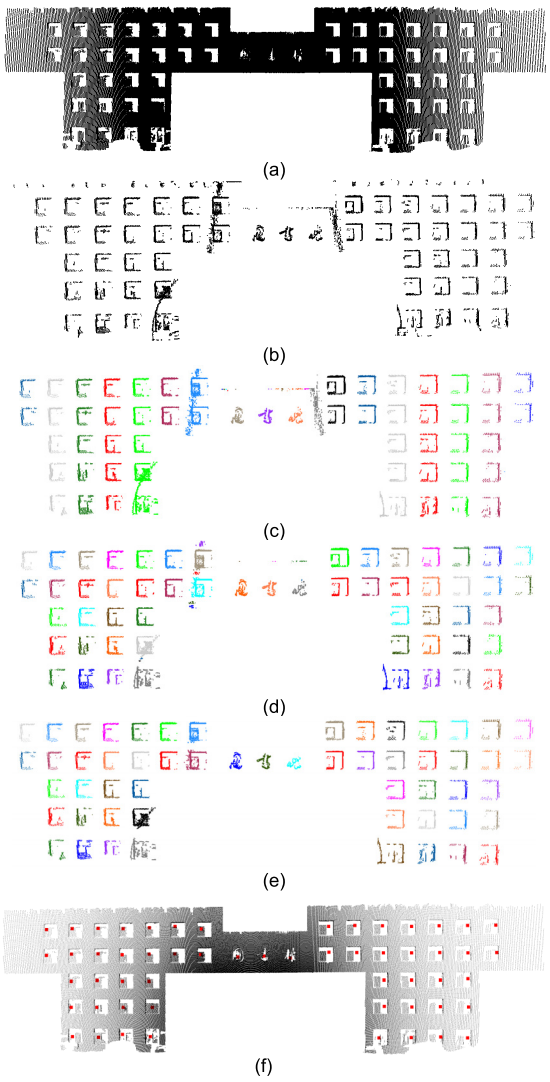

FIGURE 10. Window extraction from facade point cloud 4. (a) Facade point cloud 4. (b) The extracted salient points. (c) The vertical splitting. (d) The horizontal splitting. (e) The extracted repetitive structures. (f) The detected windows.

saliency. Fig. 9(c) and (d) show the vertical and horizontal splitting of the salient points, respectively. Fig. 9(e) shows the final window extraction result and each window is presented by a red node in Fig. 9(f). Given the input noise point clouds of a facade, our repetition splitting and extraction method automatically extracts the facade elements accurately.

Fig. 10(a) shows a library wall in Xi'an University of Technology. The windows on the facade are regularly aligned. Fig. 10(b) shows the salient points. Fig. 10(c) and (d) shows the vertical and horizontal splitting of the salient points. Fig. 10(e) shows the final repetition extraction result. The three characters on the facade are mistaken for windows. Each window is represented by a red node in Fig. 10(f).

B. COMPARISON

We qualitatively compare the splitting procedure employed in our method with Peethambaran and Wang [8]. The

FIGURE 11. Qualitative comparison. (a) The boundary points of facade point cloud 2. (b) Removing the boundary points that are close to the convex hull of facade point cloud 2. (c) The splitting result that is obtained using the method of Peethambaran and Wang [8]. (d) The boundary points of facade 3. (e) Removing the boundary points that are close to the convex hull of facade 3. (f) The splitting result that is obtained using the method of Peethambaran and Wang [8].

comparison result is presented in Fig. 11. The first row shows the boundary points of facade point clouds 2 and 3 that were extracted using alpha shape method. The second row shows the interior boundary points after removing the boundary points close to the convex hull of the facade. The splitting results that were obtained using the method of Peethambaran and Wang [8] are shown in the third row. The blue lines in Fig. 11(e) and (f) represent the splitting positions. For facade point cloud 2, the boundaries of the window are not extracted accurately using alpha shape method because the windows in the first row are not readily identifiable. The first row is split into three parts by mistake. In addition, the third and fourth rows are not separated because there is a door across the wall that spans two rows.

For facade point cloud 3, there are many noise points around the windows. Incorrect boundaries are extracted from facade point cloud 3, which lead to the improper splitting of windows. The rows of windows are not split and the last three columns are also not split.

Table 2 presents a quantitative evaluation of the window detection results for facade point clouds 2 and 3 using the method of Peethambaran and Wang [8] and our method. The columns show the number of actual counted repetitions, the number of detected repetitions, and the number of false negatives.

In extracting windows from diversified and noisy facades, our method substantially outperforms the method of

TABLE 2. Quantitative evaluation of the detection results on two datasets.

Method	Data	Count.	Detect.	F.Neg
Method of Peethambaran [8]	facade point cloud 2	31	8	23
	facade point cloud 3	20	0	20
Our method	facade point cloud 2	31	31	0
	facade point cloud 3	20	20	0

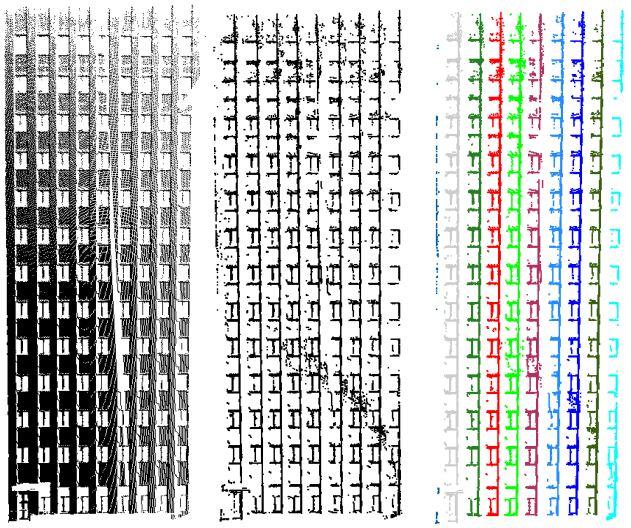

FIGURE 12. A challenging example. (a) A building facade. (b) The extracted salient points. (c) The vertical splitting result that was obtained using the proposed method.

Peethambaran and Wang [8], which extracts windows that are regularly aligned with the respective 2D axes. The saliency map construction provides an effective approach for extracting meaningful salient points from facade point clouds.

C. LIMITATIONS

Our method is not applicable to facades in which the windows are connected along the wall edge. Figure 12 (a) shows a facade with vertical wall eaves throughout the wall. In our current implementation, the extracted salient points include the vertical wall eaves that are beside window eaves. As shown in Figure 12 (b), a side edge of a window is coincident with a wall eave. Each column of windows can be segmented using the vertical splitting method(Figure 12 (c)). However, for each vertical eave, the horizontal splitting cannot generate satisfactory results due to the connection of the vertical wall eaves.

In addition, the characters on the facade that are similar in size to the window may be mistaken for windows (Figure 10(f)).

VI. CONCLUSION AND FUTURE WORK

In this paper, we construct a saliency map on 3D point clouds directly for detecting repeated structures on a facade. Our proposed algorithm was successfully applied to several facade point clouds to extract repetitive structures. Even for noisy facades, our method generates a reasonable splitting, in which each window is extracted accurately. The method avoids partitioning the facade in advance and does not require the 3D data to be projected into a 2D plane. In our algorithm, the salient points that are extracted based on the global/local saliency represent the regions of repetitions. The salient points are vertically split and, subsequently, horizontally split. A refinement is proposed for improving the repetition detection results. For some facades, the repetitions cannot be split correctly if they are connected to each other. In future work, additional geometric features should be considered to improve the detection accuracy of the proposed method.

REFERENCES

[1] X. Qin, M. Jagersand, X. Yang, and J. Wang, "Building facade recognition from aerial images using Delaunay triangulation induced feature perceptual grouping," in *Proc. IEEE Int. Conf. Pattern Recognit. (ICPR)*, Dec. 2016, pp. 3368–3373.
[2] J. Liu, E. Z. Psarakis, Y. Feng, and I. Stamos, "A kronecker product model for repeated pattern detection on 2D urban images," *IEEE Trans. Pattern Anal. Mach. Intell.*, vol. 41, no. 9, pp. 2266–2272, Sep. 2019.
[3] G. Nishida, A. Bousseau, and D. G. Aliaga, "Procedural modeling of a building from a single image," *Comput. Graph. Forum.*, vol. 37, no. 2, pp. 415–429, 2018.
[4] C.-H. Shen, S.-S. Huang, H. Fu, and S.-M. Hu, "Adaptive partitioning of urban facades," *ACM Trans. Graph.*, vol. 30, p. 184, Dec. 2011.
[5] S. M. I. Zolanvari and D. F. Laefer, "Slicing Method for curved façade and window extraction from point clouds," *ISPRS-J. Photogramm. Remote Sens.*, vol. 119, pp. 334–346, Sep. 2016.
[6] S. M. I. Zolanvari, D. F. Laefer, and A. S. Natanzi, "Three-dimensional building façade segmentation and opening area detection from point clouds," *ISPRS-J. Photogramm. Remote Sens.*, vol. 143, pp. 134–149, Sep. 2018.
[7] S. Pu and G. Vosselman, "Knowledge based reconstruction of building models from terrestrial laser scanning data," *J. Photogram. Remote Sens.*, vol. 64, no. 6, pp. 575–584, May 2009.
[8] J. Peethambaran and R. Wang, "Enhancing urban façades via LiDAR-based sculpting," *Comput. Graph. Forum.*, vol. 36, no. 8, pp. 511–528, 2017.
[9] C. H. Lee, A. Varshney, and D. W. Jacobs, "Mesh saliency," *ACM Trans. Graph.*, vol. 24, no. 3, pp. 659–666, Jul. 2005.
[10] R. Song, Y. Liu, R. R. Martin, and K. R. Echavarria, "Local-to-global mesh saliency," *Vis. Comput.*, vol. 34, no. 3, pp. 323–336, 2018.
[11] H.-K. Chen and M.-W. Li, "A novel mesh saliency approximation for polygonal mesh segmentation," *Multimedia Tools Appl.*, vol. 77, no. 13, pp. 17223–17246, 2018.
[12] E. Shtrom, G. Leifman, and A. Tal, "Saliency detection in large point sets," in *Proc. IEEE Int. Conf. Comput. Vis.*, Jun. 2013, pp. 3591–3598.
[13] F. P. Tasse, J. Kosinka, and N. Dodgson, "Cluster-based point set saliency," in *Proc. IEEE Int. Conf. Comput. Vis.*, Jun. 2015, pp. 163–171.
[14] Y. Guo, F. Wang, and J. Xin, "Point-wise saliency detection on 3D point clouds via covariance descriptors," *Vis. Comput.*, vol. 34, no. 10, pp. 1325–1338, 2017.
[15] P. Müller, G. Zeng, P. Wonka, and L. Van Gool, "Image-based procedural modeling of facades," *ACM Trans. Graph.*, vol. 26, p. 85, Aug. 2007.
[16] C. Wu, J.-M. Frahm, and M. Pollefeys, "Detecting large repetitive structures with salient boundaries," in *Proc. Eur. Conf. Comput. Vis.*, 2010, pp. 142–155.
[17] M. Mathias, A. Martinović, and L. Van Gool, "ATLAS: A three-layered approach to facade parsing," *Int. J. Comput. Vis.*, vol. 118, no. 1, pp. 22–48, 2016.
[18] Y. Lian, X. Shen, and Y. Hu, "Detecting and inferring repetitive elements with accurate locations and shapes from façades," *Vis. Comput.*, vol. 34, no. 4, pp. 491–506, 2018.
[19] H. Xiao, G. Meng, L. Wang, and C. Pan, "Facade repetition detection in a fronto-parallel view with fiducial lines extraction," *Neurocomputing*, vol. 273, pp. 435–447, Jan. 2018.

[20] A. Cohen, M. R. Oswald, Y. Liu, and M. Pollefeys, "Symmetry-aware façade parsing with occlusions," in *Proc. IEEE Int. Conf. 3D Vis.*, Oct. 2017, pp. 393–401.
[21] X. Yang, X. Qin, J. Wang, J. Wang, X. Ye, and Q. Qin, "Building façade recognition using oblique aerial images," *Remote Sens.*, vol. 7, no. 8, pp. 10562–10588, 2015.
[22] S. Friedman and I. Stamos, "Online detection of repeated structures in point clouds of urban scenes for compression and registration," *Int. J. Comput. Vis.*, vol. 102, nos. 1–3, pp. 112–128, 2013.
[23] A. Mesolongitis and I. Stamos, "Detection of windows in point clouds of urban scenes," in *Proc. IEEE Conf. Comput. Vis. Pattern Recognit. (CVPR)*, Jun. 2012, pp. 17–24.
[24] A. K. Aijazi, P. Checchin, and L. Trassoudaine, "Automatic detection and feature estimation of windows in 3D urban point clouds exploiting façade symmetry and temporal correspondences," *Int. J. Remote Sens.*, vol. 35, no. 22, pp. 7726–7748, 2014.
[25] Z. Li, L. Zhang, P. T. Mathiopoulos, F. Liu, L. Zhang, S. Li, and H. Liu, "A hierarchical methodology for urban facade parsing from TLS point clouds," *ISPRS J. Photogramm. Remote Sens.*, vol. 123, pp. 75–93, Jan. 2017.
[26] W. Hao, Y. Wang, and W. Liang, "Slice-based building facade reconstruction from 3D point clouds," *Int. J. Remote Sens.*, vol. 39, no. 20, pp. 6587–6606, 2018.
[27] H. Wang, H. Luo, C. Wen, J. Cheng, P. Li, Y. Chen, and C. Wang, "Road boundaries detection based on local normal saliency from mobile laser scanning data," *IEEE Geosci. Remote Sens. Lett.*, vol. 12, no. 10, pp. 2085–2089, Oct. 2015.
[28] R. B. Rusu, N. Blodow, and M. Beetz, "Fast point feature histograms (FPFH) for 3D registration," in *Proc. IEEE Int. Conf. Robot. Automat. (ICRA)*, May 2009, pp. 3212–3217.
[29] R. B. Rusu and S. Cousins, "3D is here: Point cloud library (PCL)," in *Proc. IEEE Int. Conf. Robot. Automat. (ICRA)*, May 2011, pp. 1–4.
[30] N. Paparoditis, B. Vallet, B. Marcotegui, and A. Serna. *Paris-Rue-Cassette Database*. Accessed: May 15 2014. [Online]. Available: http://data.ign.fr/benchmarks/UrbanAnalysis/download/Cassette_idclass.zip

WEN HAO received the B.S. and M.S. degrees from the Department of Computer Science, Shann'xi Normal University, Xi'an, China, in 2008 and 2011, respectively, and the Ph.D. degree from the Xi'an University of Technology, Xi'an, in 2015, where she is currently an Associate Professor with the Institute of Computer Science and Engineering. Her research interests include pattern recognition and computer vision.

WEI LIANG received the B.S. degree in computer science and engineering from the Huaihai Institute of Technology, in 2008, and the Ph.D. degree in computer architecture from Xidian University, in 2014. She is currently a Lecturer with the Institute of Computer Science and Engineering, Xi'an University of Technology. Her current research interests include computer graphics, multispectral image compression, and multispectral image registration.

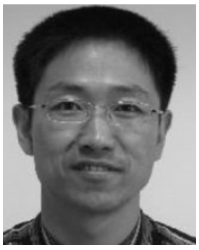

YINGHUI WANG received the Ph.D. degree from North-west University, Xi'an, China, in 2002. From 2003 to 2005, he was a Postdoctoral Fellow with Peking University, Beijing, China. He is currently a Professor with the Institute of Computer Science and Engineering, Xi'an University of Technology, China. His research interests include image analysis and pattern recognition.

MINGHUA ZHAO received the Ph.D. degree in computer science from Sichuan University, Chengdu, China, in 2006. After that, she joined Xi'an University of Technology, Xi'an, China, where she is currently a Professor with the Institute of Computer Science and Engineering. Her research interests include computer graphics, image processing, pattern recognition, and computer vision.

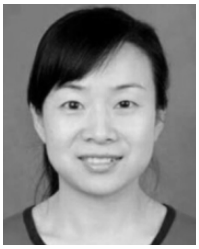

YE LI received the M.S. and Ph.D. degrees from the Xi'an University of Technology, Xi'an, China, in 2003 and 2016, respectively, where she is currently an Associate Professor with the Institute of Computer Science and Engineering. Her research interests include computer vision, image processing, and pattern recognition.